Int. J. Electrochem. Sci., 15 **(2020)** 10117 – 10128, doi: 10.20964/2020.10.70

International Journal of
ELECTROCHEMICAL
SCIENCE
www.electrochemsci.org

Sulfidation of NiCo-Layered Double Hydroxide and its Capacitance performance

Xiaolin Qiu, Chen Wen, Shuhua Bai, Junwei An*

Nanchang Institute of Technology, Nan Chang, China, 330013
*E-mail: winstonewen@126.com

Received: 17 November 2019 / *Accepted:* 4 August 2020 / *Published:* 31 August 2020

Nickel-cobalt layered double hydroxide (NC-LDH) and Na_2S were used as precursors and sulfur source, synthesizing a series of sulfurized products at different degrees by hydrothermal method. The structure of products was characterized by X-ray diffraction. The morphology of them was characterized by scanning electron microscopy (SEM) and transmission electron microscopy (TEM). The elemental content and valence of the products were characterized by X-ray photoelectron spectroscopy (XPS). Then the cyclic voltammetry (CV) and galvanostatic charge-discharge (GCD) to characterize the electrochemical performance of the products. The results show that when the sulfidation is incomplete, the product is NC-LDH/Co_9S_8 or $NiCo_2S_4$/Co_9S_8 two kinds of material, while when the sulfidation is completed, the product is only $NiCo_2S_4$. In addition, specific capacitance increases gradually with the increased degree of sulfidation.

Keywords: NiCo-layered double hydroxide; sulfidation; capacitance performance

1. INTRODUCTION

With the development of society and the increase of population, the shortage of resources and energy has become an urgent problem to be solved [1]. Therefore, the development of new energy sources and new energy storage technologies is imperative [2, 3]. Supercapacitor is a new type of energy storage which equipped with advantages of high power density, long life, wide working temperature limit, free maintenance and green and environmental protection [4]. Therefore, it has become a key research object of scholars at home and abroad.

Bimetallic hydroxides have a unique layered structure and a variable valence state, excellent tantalum capacitance characteristics and various morphologies, and have been extensively studied in the field of supercapacitors [5~10]. Enhancing its conductivity, increasing the electron transfer rate during electrochemical reactions, and improving its capacitance performance have been the focus of its research. Recently, studies have shown that the introduction of defects in metal oxides can improve conductivity. Lu et al. [11] found that the electrochemical performance of oxygen-containing hole-α-Fe_2O_3 nanowires is significantly better than that of the original α-Fe_2O_3, mainly because of the increased carrier density. Sulfides have a similar structure to oxides, and sulfur has a lower energy level than oxygen and better conductivity. Xiao's group [12] prepared tubular $NiCo_2S_4$. The research shows that its conductivity is 100 times that of $NiCo_2O_4$. When the current density is 4 mA cm^{-2}, its specific capacitance is 0.87 F cm^{-2}, and the rate is stable and cyclic. High sex. The product was subjected to ultraviolet-visible absorption spectroscopy and current-voltage testing, and it was found that the obtained sulfide had a lower optical band gap energy and a higher conductivity than the oxide. An asymmetric supercapacitor assembled with NiS as the positive electrode and graphene as the negative electrode can obtain a mass specific capacitance of 181 F g-1 at a current density of 1 A g^{-1}, 1000 charge and discharge at 2 A g^{-1} Cycle, the specific capacitance retention rate is 92% [13]. Yu et al. [14] prepared a manganese-cobalt sulfide/three-dimensional graphene composite and applied it with a supercapacitor with a specific capacitance of 1938 F g^{-1} at 5 A g^{-1}, when the current density increased to 100 A g^{-1}, the specific capacitance can maintain 76.8% of the original specific capacitance, showing excellent electrochemical performance.

Some progress has also been made in the study of bimetallic sulphides. Zhang et al. [15] hydrothermally prepared a series of $NiCo_2S_4$ with different morphologies, and found that the tubular material has the highest specific capacitance and cycle performance. After 5000 cycles of charge and discharge, the specific capacitance retention rate was 75.9%. Zhou et al. [16] found that changes in vulcanization conditions change the properties of the material during vulcanization.

In this paper, nickel-cobalt double hydroxide (NC-LDH) was used as the precursor of vulcanization, and different concentrations of $Na_2S•6H_2O$ were used as sulfur source for vulcanization treatment. The different concentrations of sulfur source were studied at the same temperature and the same reaction time. The degree of vulcanization of the body, as well as the mechanism of the effect of product vulcanization on performance.

2. EXPERIMENTAL

2.1 Vulcanization of NC-LDH

Add 1 mmol of $NiCl_2•6H_2O$, 2 mmol of $CoCl_2•6H_2O$ and 10 mmol of urea to 30 ml of deionized water, stir for 30 min on a magnetic stirrer, put into the reaction kettle, and react at 180 ° C for 12 h to obtain the sample. It was washed 3 times with deionized water, washed once with ethanol, and dried in a vacuum oven at 60 ° C for 12 hours, and the obtained pink powder was designated as NC-LDH.

Prepared by two-step hydrothermal method, NC-LDH was selected as the precursor of vulcanization. 0.0609g of the dried NC-LDH precursor was dissolved in 30ml of deionized water, stirred for 30 minutes, and 0.1g was added to the mixed solution $Na_2S•6H_2O$. After stirring evenly for 30 minutes, the final mixed brown solution was transferred to an autoclave and reacted at 160 ° C for 10 h. The black precipitate after the final reaction was centrifuged and washed 3 times with deionized water. It was washed once and finally dried in a vacuum oven at 60 ° C for 12 h, and the obtained black product was designated as NC-LDHS-1. According to the quality of the added $Na_2S{\bullet}6H_2O$, the products with the addition amount of 0.1g, 0.2g, 0.3g and 0.4g were recorded as NC-LDHS-1, NC-LDHS-2, NC-LDHS-3 and NC-LDHS-4.

2.2 Sample structure and morphology

The morphology of the material was characterized by scanning electron microscopy (SEM) and transmission electron microscopy (TEM). The model of the scanning electron microscope was 7500 field emission scanning electronic microscope. The test condition was 10 kV, 15 μA. The model of the transmission electron microscope was JEOL- 2100F, test conditions are 200 kV accelerating voltage.

The relative size of the S vacancies is characterized by X-ray photoelectron spectroscopy (XPS), model, Al-Ka X-rays.

2.3 Electrode preparation and electrochemical performance study

The electrode preparation process is as follows. A certain amount of PVDF was taken in a beaker and baked in an oven for 30 minutes. A pipette was used to take a certain amount of N-methylpyrrolidone (NMP) into a small beaker and stir for 50 minutes. The PVDF was completely dissolved in an organic solvent, and then acetylene black and NC-LDHS samples were weighed in the above mixed solution according to the ratio of NC-LDHS: acetylene black, PVDF=85:10:5 (mass ratio), and stirred well for 5 hours. The obtained mixed electrode solution was blade coated on carbon paper with a spatula and dried in a vacuum oven at 60 ° C for 12 h. Before the drawdown, the mass of the carbon paper is first weighed in order to obtain the quality of the active material for subsequent electrochemical performance testing.

The electrochemical performance test was carried out in a three-electrode system. NC-LDHS was the working electrode, Hg/HgO was the reference electrode, platinum electrode was the counter electrode, 6M KOH solution was used as the electrolyte, and Shanghai Chenhua CHI660e electrochemical workstation was tested.

Cyclic voltammetry (CV), constant current charge and discharge (GCD), and electrochemical impedance test (EIS) were performed on NC-LDHS. In the CV test, the scanning voltage range is -0.3-0.6V, and the scanning speed is 5-30 mV/s^{-1}. The GCD test conditions are, voltage range is -0.1-0.36V, current density is 1, 2, 3, 5 and 10 A g^{-1}. The EIS test conditions are: at an open circuit potential, the frequency is 0.01-100 kHz.

The value of the specific capacitance is calculated by the formula (1) [17]:

$$C_m = \frac{C}{m} = \frac{i \times \Delta t}{\Delta V \times m} \qquad (1)$$

Where i(A) discharge current, Δt(s) is the discharge time and ΔV(V) is the potential window.

3. RESULTS AND DISCUSSION

3.1 X-ray diffraction analysis

In order to characterize the structural characteristics of the double metal hydroxides of different degrees of vulcanization, the sulfide products were subjected to XRD tests and the results are shown in Fig. 1. As can be seen from the figure, the characteristic peaks of NC-LHDS-1, NC-LHDS-2, NC-LHDS-3, and NC-LHDS-4 changed significantly compared to NC-LDH. Compared with $Co(CO_3)0.5OH\bullet0.11H_2O$ standard card (PDF#48-0083), the characteristic peak of NC-LDH corresponds to one-to-one, and the crystal plane corresponding to 30.441°, 35.480° and 44.669° is (300), 040) and (050). Comparing the $NiCo_2S_4$ standard map (PDF#20-0782), the characteristic peaks of NC-LHDS-4 correspond to one-to-one, and the crystal planes corresponding to 31.586°, 38.319° and 55.33° are (311), (400) and (440). Compared with NC-LDHS-4, incompletely sulfurized NC-LDHS-1, NC-LDHS-2 and NC-LDHS-3 have some impurity peaks. After characterization, the impurity peak corresponds to Co_9S_8. The results show that when the sulfidation is incomplete, there is production of Co_9S_8. In NC-LDHS-1, the product composition is NC-LDH/Co_9S_8. In NC-LDHS-2 and NC-LDHS-3, the product composition is mainly $NiCo_2S_4$/Co_9S_8. In NC-LDHS-4, the product composition is NiCo2S4. Studies [18~20] have shown that the presence of Co_9S_8 is due to incomplete vulcanization caused by Na_2S as a sulfur source. This impurity can be eliminated by increasing the concentration of the sulfur source.

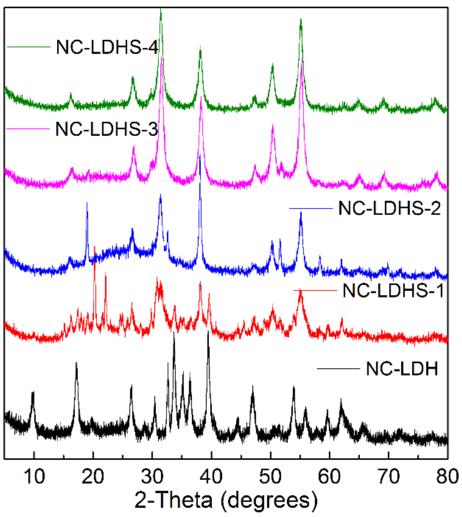

Figure 1. XRD patterns of NC-LDH, NC-LDHS-1, NC-LDHS-2, NC-LDHS-3 and NC-LDHS-4

3.2 Scanning electron microscopy and transmission electron microscopy analysis

Figure 2 is an SEM image of NC-LDH, NC-LDHS-1, NC-LDHS-2, NC-LDHS-3 and NC-LDHS-4, respectively. As can be seen from Figure 2(a), NC-LDH- 180-12 is a sea urchin composed of nanoneedles. With the addition of Na2S, the morphology of the product gradually changed. When 0.1g

Na_2S is added, the SEM of NC-LDHS-1 is shown in Fig. 2(b). It can be seen that there are many small particles on the surface of the nanoneedle, and some changes have taken place in the morphology. When the amount of Na_2S added is increased to 0.2 g, the SEM of NC-LDHS-2 is shown in Fig. 2(c). The nanoneedle starts to become shorter, the size is reduced by 7μm To 4μm. The white matter accumulated on the surface gradually increases, but the overall morphology does not change significantly. When the amount of Na_2S added is increased to 0.3 g, the SEM of NC-LDHS-3 is shown in Fig. 2(d). The shape of the urchin is gradually disintegrated and the nanoneedle is gradually changed into a smaller size nanosheet. Finally, when the amount of Na_2S added is increased to 0.4g, the vulcanization is complete. When the product is $NiCo_2S_4$, the morphology changes greatly and the nanoneedle is converted into finely divided nanosheets.

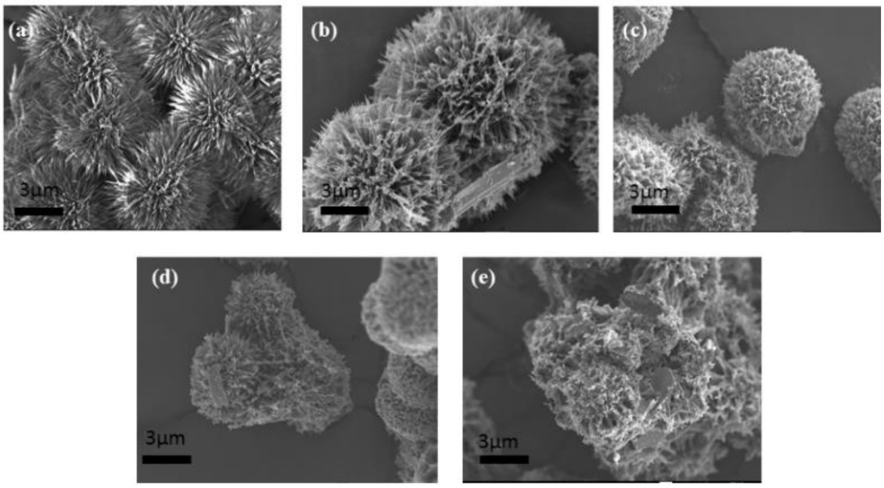

Figure 2. SEM images of (a) NC-LDH, (b) NC-LDHS-1, (c) NC-LDHS-2, (d) NC-LDHS-3 and (e) NC-LDHS-4

Figure 3 is a TEM image of NC-LDHS-1 at different magnifications. As can be seen from the figure, NC-LDHS-1 has a nanoneedle structure, and the diameter of the nanoneedle is about 10 nm. Fig. 3(b) is a high-resolution TEM image of NC-LDHS-1. By calculation, the interplanar spacing of the crystal faces is 2.85 Å, which is consistent with the (300) interplanar spacing in NC-LDH in XRD.

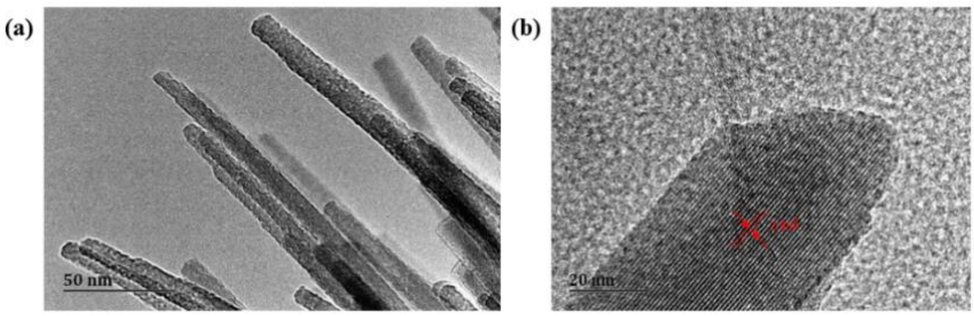

Figure 3. TEM images of NC-LDHS-1at (a) low magnification and (b) high magnification

3.3 X-ray photoelectron spectroscopy

X-ray photoelectron spectroscopy Figure 4 shows the XPS spectra of S 2p for NC-LDHS-1, NC-LDHS-3 and NC-LDHS-4. The peak at low energy level corresponds to S 2p 3/2, which is a typical metal - Characteristic peak of sulfur bond [12, 21]. Corresponding to the high energy level is S 2p 1/2, which is used to characterize the concentration of sulfur holes in the product [22]. It can be seen from the spectrum of XPS that as the degree of vulcanization increases, the area of the S 2p 1/2 peak gradually increases. It can be calculated from the calculation that in NC-LDHS-1, the concentration of sulfur holes is 38.83%, in NC. In LDHS-3, the concentration of sulfur holes was 52.00%, and in NC-LDHS-4, the concentration of sulfur holes was 53.03%.

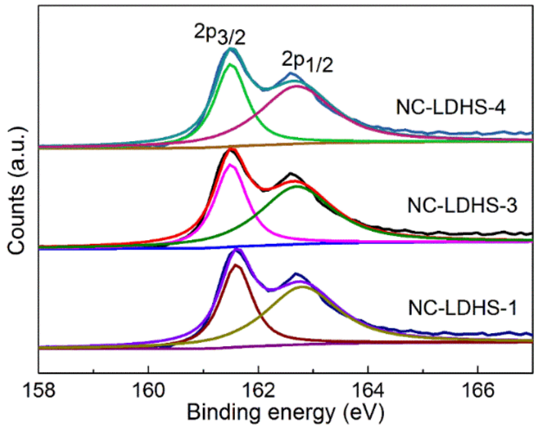

Figure 4. S 2p XPS spectrum of NC-LDHS-1, NC-LDHS-3 和 NC-LDHS-4

3.4 Study on electrochemical properties of sulfurized products

In order to characterize the electrochemical performance of NC-LDHS, CV and GCD tests were performed on NC-LDHS. The results are shown in Figures 5-7. Figure 5(a) shows the CV curves of NC-LDHS-1, NC-LDHS-2, NC-LDHS-3, and NC-LDHS-4 at 10 mV s^{-1}. As can be seen from the figure, all the curves are shown. Both have redox peaks, indicating that NC-LDHS has significant tantalum capacitance performance. Comparing the four curves, as the degree of vulcanization increases, the area of the CV curve gradually increases, indicating that the capacitance performance is gradually increased. The electrochemical reactions (Ni^{2+}/Ni^{3+} and $Co^{2+}/Co^{3+}/Co^{4+}$) occurring in the electrolyte can be expressed by the following equation [23]:

$$NiCo_2S_4 + OH^- + H_2O \leftrightarrow NiS_{4-4x}OH + 2CoS_{2x}OH + e^- \quad (2)$$

$$CoS_{2x}OH + OH^- \leftrightarrow CoS_{2x}O + H_2O + e^- \quad (3)$$

$$CoS_{2x} + OH^- \leftrightarrow CoS_{2x}OH + e^- \quad (4)$$

$$NiS_{4-4x} + OH^- \leftrightarrow NiS_{4-4x}OH + e^- \quad (5)$$

Figure 5 (b) is a charge-discharge curve of NC-LDHS-1, NC-LDHS-2, NC-LDHS-3, and NC-LDHS-4 at 1 A g^{-1}. As can be seen from the figure, as the degree of vulcanization increases, the specific capacitance gradually increases. According to the calculation formula of specific capacitance, the specific capacitances of NC-LDHS-1, NC-LDHS-2, NC-LDHS-3 and NC-LDHS-4 at 1 A g^{-1} current density are

598.7, 993.8, 1273.04 and 2006.8 F g^{-1}. Compared to NC-LDH (583.3 F g^{-1}), the specific capacitance of the nickel-cobalt double hydroxide after vulcanization is increased.

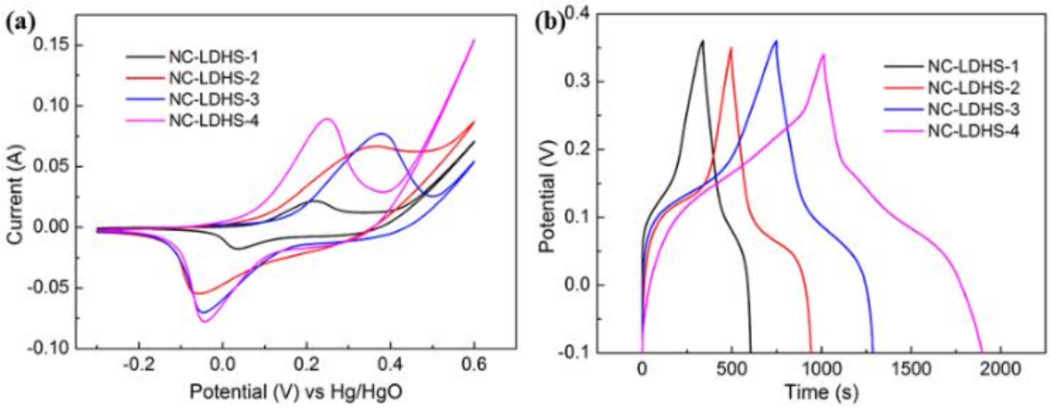

Figure 5. (a) CV curves of NC-LDHS-1, NC-LDHS-2, NC-LDHS-3 and NC-LDHS-4 at the scan rate of 10 mV s^{-1}; (b) GCD curves of NC-LDHS-1, NC-LDHS-2, NC-LDHS-3 and NC-LDHS-4 at the current density of 1 A g^{-1}

This is mainly because after the vulcanization, the conductivity is increased, the sulfur holes replace the oxygen holes of the original nickel-cobalt double metal hydroxide, and the sulfur holes have better conductivity and capacitance properties than the oxygen holes. Moreover, as the concentration of the sulfur source increases, the concentration of sulfur holes also gradually increases, and the specific capacitance performance increases.

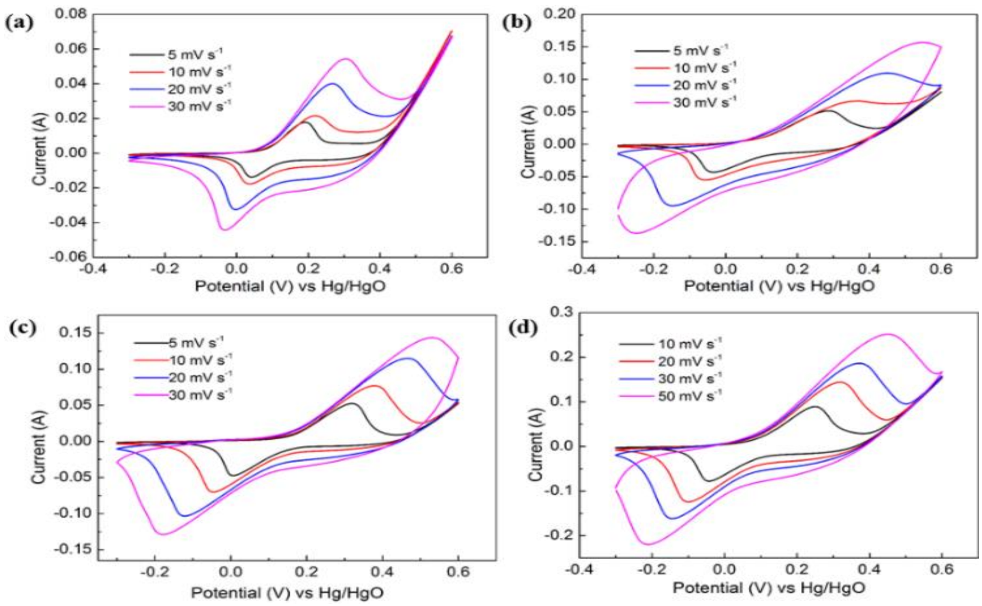

Figure 6. CV curves of (a) NC-LDHS-1, (b) NC-LDHS-2, (c) NC-LDHS-3 and (d) NC-LDHS-4 at different scan rate

Figure 6 shows the CV curves of NC-LDHS at different scan rates. It can be seen from the figure that all the curves have obvious redox peaks, which proves that NC-LDHS has better tantalum capacitance performance. As the scan rate increases, all of the curves remain in their original shape, with only partial polarization occurring.

Figure 7 is the charge-discharge curve of NC-LDHS at different current densities. All the curves have obvious tantalum-capacitance platform and have very good symmetry. With the increase of current density, the shape of charge-discharge curve does not change significantly. Explain that the material has high rate performance. Figure 7(a) shows the charge-discharge curve of NC-LDHS-1. According to the calculation formula of specific capacitance (1), the current density of NC-LDHS-1 at 1, 2, 3, 5 and 10 A g^{-1} can be calculated. The lower specific capacitances are 598.7, 583.6, 576, 554.4 and 502.2 F g^{-1}, respectively, and when the current density is increased to 10 A g^{-1}, the original specific capacitance can still be maintained at 83.89%. Figure 7(b) is the charge-discharge curve of NC-LDHS-2. According to the calculation formula of specific capacitance (1), the current density of NC-LDHS-1 at 1, 2, 3, 5 and 10 A g^{-1} can be calculated. The specific capacitances are 993.8, 992.7, 988.7, 923.9 and 858.51 F g^{-1}, respectively. When the current density is increased to 10 A g^{-1}, the specific capacitance can still maintain 86.39% of the original specific capacitance. Figure 7(c) is the charge-discharge curve of NC-LDHS-3. According to the calculation formula of specific capacitance (1), the current density of NC-LDHS-1 at 1, 2, 3, 5 and 10 A g^{-1} can be calculated.

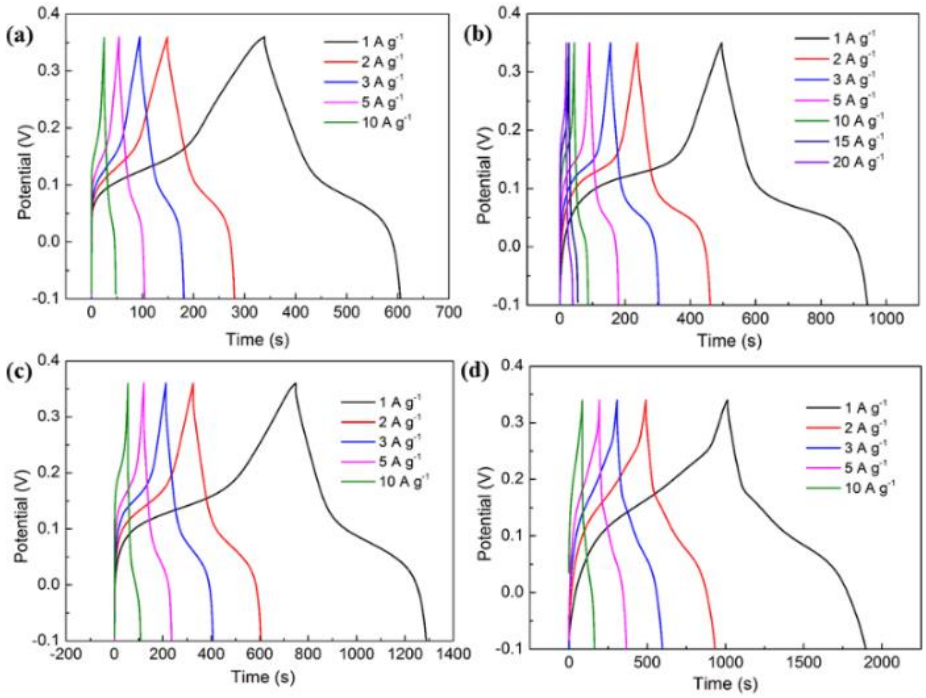

Figure 7. GCD curves of (a) NC-LDHS-1, (b) NC-LDHS-2, (c) NC-LDHS-3 and (d) NC-LDHS-4 at different current density

The specific capacitances below are 1273.1, 1240.2, 1215.65, 1194.3, and 1121.7 F g^{-1}. When the current density is increased to 10 A g^{-1}, the specific capacitance can still maintain 88.09% of the original specific capacitance. Figure 7(d) is the charge-discharge curve of NC-LDHS-4. According to the calculation formula of specific capacitance (1), the current density of NC-LDHS-1 at 1, 2, 3, 5 and 10 A g^{-1} can be calculated. The specific capacitances are 2006.8, 2004.6, 1979.3, 1967.1, and 1804.6 F g^{-1}, respectively. When the current density is increased to 10 A g^{-1}, the specific capacitance can still maintain 89.92% of the original specific capacitance. When the concentration of sulfur source increases, not only the performance of the capacitor increases, but also the rate performance increases from 83.89% to 89.92%. When the sulfur source concentration is relatively low, the nickel-cobalt double metal hydroxide is incompletely vulcanized, and the presence of Co_9S_8 impurities increases the introduction of additional interfaces and interfaces, hindering electron transfer in the material. As the concentration of the sulfur source increases, the impurities gradually disappear, and the sulfur vacancies provide an excess of carriers as electron donors, thereby increasing the conductivity of the NC-LDHS.

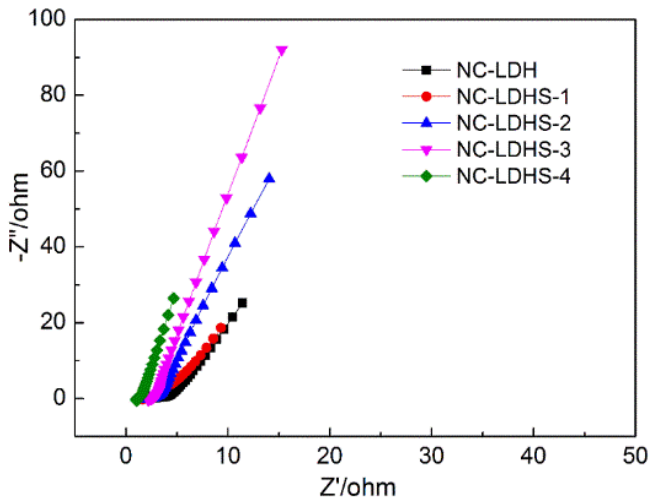

Figure 8. Nyquist plots of NC-LDH, NC-LDHS-1, NC-LDHS-2, NC-LDHS-3 and NC-LDHS-4

Table 1. Fitted results by Zsimpwin of Nyquist plots of NC-LDH, NC-LDHS-1, NC-LDHS-2, NC-LDHS-3 and NC-LDHS-4

Specimens	NC-LDH	NC-LDHS-1	NC-LDHS-2	NC-LDHS-3	NC-LDHS-4
$R_{ct}(\Omega.cm^2)$	1105	892.70	620.7	550.5	375.5
Z_w(S/S0.5)	0.002154	0.001877	0.001495	0.001313	0.001245

3.5 Electrochemical impedance spectroscopy analysis of sulfurized products

The Nyquist curves for NC-LDH and NC-LDHS are shown in Figure 8, consisting of a semicircle and an oblique line. The diameter of the semicircle in the high frequency region corresponds to the charge transfer resistance (R_{ct}). The smaller the diameter, the smaller the R_{ct}; the magnitude of the Warburg impedance (Z_W) is related to the line corresponding to the low frequency at a certain angle to the real axis, indicating The impedance of the ion transport in the electrolyte, the greater the slope of the line, the smaller the ZW [24-30]. It can be seen from the figure that the R_{ct} of NC-LDH, NC-LDHS-1, NC-LDHS-2, NC-LDHS-3 and NC-LDHS-4 is gradually reduced, mainly due to the increase of sulfur holes. The conductivity of the material is increased; the Z_W impedance is also reduced, mainly because the product structure becomes loose as the degree of vulcanization increases, which is beneficial to the electrolyte infiltration and ion transport.

3.6 The comparison between the material and similar electrode materials for supercapacitors

It can be known from the above the results. The specific capacitance performance and rate performance increase gradually with the increase of the degree of vulcanization. So that NC-LDHS-4 is equipped with better capacitance performance and rate performance compared with other sulfurized products. In order to evaluate the performance of NC-LDHS-4 further on, a new table was made to make comparison the material with similar electrode materials for supercapacitors that were described in literature. The results are shown in Table 2.

Table 2. performance comparison between the material and similar electrode materials for supercapacitors

Specimens (Research team)	α-Fe_2O_3 nanostructures (Lu X [11])	$NiCo_2S_4$ (Xiao J [12])	NiS (Yu M [13])	$NiCo_2S_4$ (Zhang Y [15])	NC-LDHS-4
current density(condition)	5 A g^{-1}	4 mA cm^{-2}	1 A g^{-1}	3 A g^{-1}	1 A g^{-1}
specific capacitance	348 F g^{-1}	0.87 F cm^{-2}	181 F g^{-1}	1048 F g^{-1}	2006.8 F g^{-1}

According to the Table 2, it can be known that different electrode materials have different current density. The reason why NC-LDHS-4 is provided with higher specific capacitance at certain current density compared with other similar electrode materials for supercapacitors is mainly because after the vulcanization, the conductivity is increased, the sulfur holes replace the oxygen holes of the original nickel-cobalt double metal hydroxide, and the sulfur holes have better conductivity and capacitance properties than the oxygen holes. Moreover, as the concentration of the sulfur source increases, the concentration of sulfur holes also gradually increases, and the specific capacitance performance increases.

4. CONCLUSION

In this paper, NC-LDH-180-12 is used as a precursor, and nickel-cobalt double-metal hydroxide is vulcanized to varying degrees. When the vulcanization is incomplete, the product is NC-LDH/Co_9S_8 or $NiCo_2S_4$/Co_9S_8. After the vulcanization is completed, the product is only $NiCo_2S_4$. As the degree of vulcanization increases, the urchin-like structure composed of nano-needle gradually becomes a fluffy structure composed of small nano-sheets. The results of electrochemical tests show that the specific capacitance performance and rate performance increase gradually with the increase of the degree of vulcanization. NC-LDHS-1, NC-LDHS-2, NC-LDHS-3 and NC-LDHS-4 are at 1 A g^{-1}. The specific capacitance at 1 A g^{-1} current density is 598.7, 993.8, 1273.04 and 2006.8 F g^{-1}, respectively. When the current density is increased to 10 A g^{-1}, NC-LDHS-1, NC-LDHS-2, NC-LDHS-3 and NC-LDHS-4 can still maintain 83.89%, 86.39%, 88.09% and 89.92% of the original specific capacitance. The improvement of the capacitance performance is mainly due to the increase of the concentration of sulfur holes in the product, which improves the conductivity of the material. The structure is gradually loose, which is beneficial to the electrolyte infiltration and ion transport.

References

1. L.L. Zhang and X.S. Zhao, *Chem. Soc. Rev.*, 38 (2009) 2520.
2. P. Simon and Y. Gogotsi, *Nat. Mater.*, 7 (2008) 845.
3. H.S. Chen, T.N. Cong, W. Yang, C.Q. Tan, Y.L. Li and Y.L. Ding, *Prog. Nat. Sci.*, 19 (2009) 291.
4. J.R. Miller and P. Simon, *Sci.*, 321(2008) 651.
5. M.Q. Zhao, Q. Zhang, J.Q. Huang and F. Wei, *Adv. Funct. Mater.*, 22 (2012) 675.
6. M. Yu, R.L. Liu, J.H. Liu, S.M. Li and Y.X. Ma, *Small*, 13 (2017) 1702616.
7. Y.L. Niu, R.Y. Li and Z.J. Li, *Electrochim. Acta*, 94 (2013) 360.
8. Y.W. Cheng, H.B. Zhang, C.V. Varanasi and J. Liu, *Energy Environ. Sci.*, 6 (2013) 3314.
9. Y. Bai, W.Q. Wang, R.R. Wang, J. Sun and L. Gao, *J. Mater. Chem. A*, 3 (2015) 12530.
10. Z. Gao, C. Bumgardner, N.N. Song, Y.Y. Zhang, J.J. Li and X.D. Li, *Nat. Commun.*, 7 (2016) 11586.
11. X.H. Lu, Y.X. Zeng, M.H. Yu, T. Zhai, C.L. Liang, S.L. Xie, M.S. Balogun and Y.X. Tong, *Adv. Mater.*, 26 (2014) 3148.
12. J.W. Xiao, L. Wan, S.H. Yang, F. Xiao and S. Wang, *Nano Lett.*, 14 (2014) 831.
13. A. Singh, A.J. Roberts, R.C.T. Slade and A. Chandra, *J. Mater. Chem. A*, 2 (2014) 16723.
14. M. Yu, X.J. Li, Y.X. Ma, R.L. Liu, J.H. Liu and S.M. Li, *Appl. Surf. Sci.*, 396 (2017) 1816.
15. Y.F. Zhang, M.Z. Ma, J. Yang, C.C. Sun, H.Q. Su, W. Huang and X.C. Dong, *Nanoscale*, 6 (2014) 9824.
16. F. Lu, M. Zhou, W.R. Li, Q.H. Weng, C.L. Li, Y.M. Xue, X.F. Jiang, X.H. Zeng, Y. Bando and D. Golberg, *Nano Energy*, 26 (2016) 313.
17. J.W. Chen, X. Wang, J.X. Wang and P.S. Lee, *Adv. Energy Mater.*, 6 (2016) 1501745.
18. H.C. Chen, J.J. Jiang, L. Zhang, H.Z. Wan, T. Qi and D.D. Xia, *Nanoscale*, 5 (2013) 8879.
19. J. Pu, F.L. Cui, S.B. Chu, T.T. Wang, E.H. Sheng and Z.H. Wang, *ACS Sustainable Chem. Eng.*, 2 (2013) 809.
20. L. Fei, B.P. Williams, S.H. Yoo, J.M. Carlin and Y.L. Joo, *Chem. Commun.*, 52 (2016)1501.
21. H.C. Chen, J.J. Jiang, L. Zhang, H.Z. Wan, T. Qi and D.D. Xia, *Nanoscale*, 5 (2013) 8879.
22. J.M. Duhart, M.J. Leone and N. Paladino, *Phys. Rev. B: Condens. Matter*, 70 (2004) 195404.
23. C.Y. Chen, Z.Y. Shih, Z. Yang and H.T. Chang, *J. Power Sources*, 215 (2012) 43.
24. M. Yu, J.P. Chen and Y.X. Ma, *Appl. Surf. Sci.*, 314 (2014) 1000.

25. Z. Gao, N.N. Song and X.D. Li, *J. Mater. Chem. A* , 3 (2015) 14833.
26. C. Guan, J.P. Liu, C.W. Cheng, H.X. Li, X.L. Li, W.W. Zhou, H. Zhang and H.J. Fan, *Energy Environ. Sci.*, 4 (2011) 4496.
27. Z.J. Fan, J. Yan, T Wei, L.J. Zhi, G.Q. Ning, T.Y. Li and F. Wei, *Adv. Funct. Mater.*, 21 (2011) 2366.
28. P.S. Santosh and Corros, *Sci*., 169 (2020) 1.
29. C.M. Samuel and G. Paul, *J. Electroanal. chem.*, 871 (2020) 114305.
30. M. Oldenburger, B. Bedurftig and A. Gruhle, F. Grimsmann, E. Richter, R. Findeisen, A. Hintennach, *J. Storage Mater.*, (2019) 272 .
31. G. Yilmaz, K.M. Yam, C. Zhang, H.J. Fan and G.W. Ho, Ad*v. Mater.*, 29 (2017) 1606814.
32. X.Q. Cai, X.Q. Shen and L.B. Ma, *Chem. Eng. J.,* 268(2020) 256.